Towards a better representation of the solar cycle in general circulation models

K. M. Nissen, K. Matthes, U. Langematz, B. Mayer

Atmos. Chem. Phys. Discuss., 7, 45–64, 2007
www.atmos-chem-phys-discuss.net/7/45/2007/

Atmospheric Chemistry and Physics Discussions

Towards a better representation of the solar cycle in general circulation models

K. M. Nissen[1], **K. Matthes**[1,2], **U. Langematz**[1], **and B. Mayer**[3]

[1]Institut für Meteorologie, Freie Universität Berlin, Carl-Heinrich-Becker-Weg 6–10, 12165 Berlin, Germany
[2]National Center for Atmospheric Research, 3450 Mitchell Lane, Boulder, CO 80301, USA
[3]Institut für Physik der Atmosphäre, Deutsches Zentrum für Luft- und Raumfahrt, Oberpfaffenhofen, Germany

Received: 17 November 2006 – Accepted: 13 December 2006 – Published: 3 January 2007

Correspondence to: K. M. Nissen (katrin.nissen@met.fu-berlin.de)

Abstract

It is shown that a high-resolution short-wave (SW) heating rate parameterization is necessary to simulate solar cycle variations in atmospheric models. The improved Freie Universität Berlin (FUB) high-resolution radiation scheme (FUBRad) is introduced and compared to the 4-band ECHAM5 SW radiation scheme of Fouquart and Bonnel (FB). Both schemes are validated against the detailed radiative transfer model libRadtran. FUBRad produces realistic heating rate variations during the solar cycle and a temperature response that is in good agreement with observations. The SW heating rate response with the FB scheme is about 20 times smaller than with FUBRad and cannot produce the observed temperature signal.

Comparison of the total short-wave heating rates under moderate solar conditions shows good agreement between FUBRad, FB and libRadtran up to 80 km indicating that both parameterizations are well suited for climate integrations that do not take solar variability into account.

The FUBRad scheme has been implemented as a sub-submodel of the Modular Earth Submodel System (MESSy).

1 Introduction

Understanding solar variability effects on climate is an important topic in current studies with state-of-the-art chemistry-climate models (CCMs). If it is possible to understand the influence of solar variability on climate, the contribution of anthropogenic effects to climate change can be better estimated. Variations in the total solar irradiance (TSI) over the 11-year solar cycle are small (0.08%) (e.g. Fröhlich, 2000) and therefore cannot be the cause for the observed changes in Earth's surface temperature. However, variations in the ultraviolet (UV) part of the solar spectrum, which is important for ozone production and middle atmosphere heating, range from 8% at 200 nm to about 5% from 220 nm to 260 nm, 0.5% around 300 nm, and 0.1% above 400 nm (e.g. Lean et

ACPD

7, 45–64, 2007

al., 1997; Woods and Rottman, 2002). Much larger variations are observed at shorter wavelengths (over 50% at 120 nm, 10–15% from 140–200 nm), which are mainly absorbed in the higher atmosphere (mesosphere and thermosphere).

As has been shown in past modeling studies (e.g. Brasseur, 1993; Haigh, 1994; Fleming et al., 1995), 11-year solar UV irradiance variations have a direct impact on the radiation and ozone budget of the middle atmosphere. In order to account for these changes a model needs to include spectrally resolved solar irradiance changes as well as ozone changes due to enhanced photo-chemical production (e.g. Larkin et al., 2000). According to a recent study by Shibata and Kodera (2005) the solar forcing is linearly composed of UV and ozone changes. In the annual mean the UV forcing is dominant and over twice as large as the ozone forcing around the stratopause and above, while the ozone forcing is dominant below 5 hPa where the UV forcing is negligible. At summer solstice however, the ozone forcing in the polar upper stratosphere reaches the same magnitude as the UV forcing (Langematz and Matthes, in preparation). Matthes et al. (2003) showed that general circulation models (GCMs) considering spectral variations between different phases of the 11-year solar cycle show a clear direct solar signal in the temperature and circulation of the upper stratosphere. These studies clearly demonstrate that the wavelengths important for ozone absorption need to be taken properly into account for solar variability studies.

During solar maximum (hereafter: solar max) years the solar UV irradiance is enhanced, which leads to additional ozone production and heating in the stratosphere and above. By modifying the meridional temperature gradient the heating can alter the propagation properties for planetary and smaller-scale waves that drive the global circulation. Thus the relatively weak, direct radiative forcing of the solar cycle in the upper stratosphere could lead to a larger indirect dynamical response in the lower atmosphere through a modulation of the polar night jet and the Brewer-Dobson circulation (Kodera and Kuroda, 2002). This has recently been confirmed in a GCM study by Matthes et al. (2004) who ascribed the successful simulation of solar variability effects in their GCM partly to the high-resolution short-wave (SW) radiation scheme and

partly to the prescription of realistic equatorial winds throughout the stratosphere. The transfer of the solar signal from the stratosphere to the troposphere is subject of current model and observational studies and includes a modulation of the Arctic oscillation (AO) at middle to high latitudes (Kodera, 2002; Matthes et al., 2006) and changes in vertical motion and precipitation in the tropics (e.g. Kodera, 2004; Haigh et al., 2005, Matthes et al., 2006). Such dynamical changes can feedback on the chemical budget of the atmosphere because of the temperature dependence of the chemical reaction rates and transport of chemical species.

In order to simulate the dynamical and chemical feedback mechanisms associated with solar irradiance variations it is essential to calculate the direct, relatively weak radiative forcing in the upper stratosphere as accurate as possible. This requires radiation codes with sufficient spectral resolution in the SW bands. However, for computational efficiency most GCMs use radiation schemes with only a few spectral intervals to calculate SW heating rates.

The aim of this paper is to demonstrate that a high-resolution SW radiation parameterization is needed for studying solar variability effects on climate. We first introduce in Sect. 2 such a high-resolution scheme, the FUBRad SW radiation parameterization for the middle atmosphere (MA). The code has been implemented into the ECHAM5/MESSy climate model (Roeckner et al., 2003; Jöckel et al., 2005) as a sub-submodel, more specifically as a submodel of the MESSy submodel RAD4ALL, which represents the standard ECHAM5 radiation scheme in a MESSy conform implementation. In Sect. 3 we validate the FUBRad scheme against the original ECHAM5 SW radiation scheme and a detailed radiative transfer model. In Sect. 4 the impact of 11-year variations in solar UV irradiance on the SW radiation balance is studied for the FUBRad and ECHAM5 schemes while Sect. 5 shows the corresponding temperature responses. In Sect. 6 the results are discussed and summarized.

2 The FUBRad scheme

The FUBRad scheme has been designed for use in a middle atmosphere (MA) GCM. It operates in the stratosphere and mesosphere between 70 and 0.01 hPa (18 and 80 km) and takes the relevant radiative processes in this altitude range into account. FUBRad has been updated from the version described in Matthes et al. (2004). It uses 49 spectral intervals in the UV and visible (VIS) part of the spectrum (121.56–680 nm). Absorption by ozone (O_3) is calculated using spectral irradiances and absorption cross sections suggested by WMO (1986) and Sander et al. (2003). Heating by molecular oxygen (O_2) in the Schumann-Runge bands and continuum is calculated using the approach of Strobel (1978). The contribution of the Lyman-α line is parameterized using effective cross sections depending on the O_2 slant column as suggested by Chabrillat and Kockarts (1997). The energy of absorbed photons is not completely converted to thermal energy, but can also be stored as chemical energy, or be emitted as airglow. Energy losses due to airglow are accounted for by using the efficiency factors of Mlynczak and Solomon (1993) for the Lyman-α line, the Hartley bands and the Schumann-Runge continuum. Conversion into chemical energy is considered in the Schumann-Runge bands and continuum as suggested by Strobel (1978). As FUBRad operates in the MA (well above the cloud level), backscattering of solar radiation is considered only for O_3 in the Chappuis and Huggins bands by Strobel (1978). FUBRad can be run both as offline model and as interactive submodel of the ECHAM5/MESSy climate model system (Jöckel et al., 2005).

To obtain UV/VIS heating rates for the full vertical domain of the GCM (including the troposphere), FUBRad has been coupled at 70 hPa to the SW radiation parameterization of Fouquart and Bonnel (1980) (FB) which is the standard SW radiation scheme in the ECHAM5 GCM (Roeckner et al., 2003). The FB scheme resolves only one spectral interval in the UV/VIS part of the spectrum (250–680 nm) but takes scattering processes on clouds into account which are important in the troposphere.

To obtain solar heating rates for the full solar spectrum (including the near-infrared,

NIR) FUBRad uses NIR-heating rates derived from the FB parameterization in 3 spectral intervals between 680 and 4000 nm at all levels. In the NIR O_3, H_2O, CO_2, CH_4, N_2O, CO and O_2 are taken into account. Aerosols and cloud particles are considered at all intervals.

FUBRad calculates SW heating rates every time step.The code has been optimized for the implementation into the ECHAM5/MESSy model and uses about 7% of the total computing time of the basic model system.

3 Validation

To validate the FUBRad radiation scheme we compare SW heating rates calculated by FUBRad with those from the standard ECHAM5 SW radiation code and from a detailed radiative transfer code, libRadtran (Mayer and Kylling, 2005). The ECHAM5 SW radiation code is based on the FB parameterization for the UV/VIS and NIR parts of the solar spectrum. The major difference to FUBRad is the UV/VIS spectral resolution, with 49 intervals in FUBRad compared to only one broad interval in ECHAM5.

libRadtran is operated in line-by-line mode for this application. O_3 and O_2 absorption cross sections had to be extended down to 120 nm. This was done following the recommendations by the International Union of Pure and Applied Chemistry (IUPAC) (Atkinson et al., 2004). O_2 absorption for the additional spectral regions was compiled from a variety of sources: The Schumann-Runge continuum follows Ogawa and Ogawa (1975) between 108 and 160 nm and Yoshino et al. (2005) between 160 and 175 nm. In the Lyman-α region, 121.4–121.9 nm, high-resolution data from Lewis (1983) is used. Temperature-dependent cross sections in the Schumann-Runge bands (175–205 nm) are taken from Minschwaner et al. (1992). The recommended Herzberg continuum from Yoshino et al. (1988) is added to the Schumann-Runge spectral lines. The same source provides the Herzberg continuum in the wavelength range 205–240 nm. O_3 absorption cross sections are temperature-dependent above 185 nm (Molina and Molina, 1986). Below 185 nm, temperature-independent data from Ackerman (1971) is used.

To completely resolve all relevant spectral features, more than 10 000 wavelengths are included between 121.4 nm and 680 nm, with a step of 0.001 nm in the Lyman-α region, 0.003 nm in the Schumann-Runge bands, and otherwise 0.1 nm below 400 nm and 1 nm above 400 nm. The spectral shape of the extraterrestrial irradiance in the Lyman-α region (121.4–121.9 nm) has been adopted from Chabrillat and Kockarts (1997). The radiative transfer is solved with the accurate disort method by Stamnes et al. (1988).

Calculations for all models were performed with profiles of pressure, temperature, oxygen, and ozone concentrations taken from the Midlatitude Summer atmosphere by (Anderson et al., 1986).

Figure 1 shows an example for the SW heating rates, integrated over the spectral interval 121–680 nm, for January 15th at the equator. The NIR is omitted as FUBRad and ECHAM5 use identical parameterizations for this interval and its contribution to the total SW heating rate in the MA is relatively small. The figure contains two profiles for the FUBRad scheme. The curve denoted FUBRad-TOTAL shows the heating rates obtained by converting the energy of each absorbed photon into thermal energy. This version is consistent with the treatment of absorbed energy in libRadtran and in the FB scheme. The profile marked FUBRad-NET shows the net SW heating rates that take into account that in the real upper atmosphere part of the energy is stored as chemical energy or emitted as airglow. This is the configuration of the code we use for our solar cycle studies. Up to 1 hPa there is close agreement between all codes. Maximum SW heating occurs at the stratopause and reaches about 10 K/day at the equator in January. Above 0.1 hPa libRadtran and FUBRad show considerably larger heating rates than the ECHAM5 code. This is due to the fact, that in contrast to FUBRad and libRadtran, the ECHAM5 scheme does not consider absorption by O_2, which dominates in the upper mesosphere. Nevertheless, the comparison with the line-by-line radiation model shows that both parameterizations (FB and FUBRad) capture SW heating rates well enough to allow realistic climate simulations up to 0.01 hPa, which is the model top of the MA version of the ECHAM5 model.

4 Solar cycle effect on SW heating rates

To study the influence of variations in UV irradiance during the 11-year solar cycle, we have calculated zonal-mean, daily-mean short-wave heating rates with the offline versions of the FUB and ECHAM5 radiation codes. Standard input data recommended by the CCMVal project (http://www.pa.op.dlr.de/CCMVal/index.html) were used including zonal-mean temperature, O_3 (Fortuin and Langematz, 1994) and H_2O distributions. CO_2, CH_4, N_2O and CFCs are uniformly mixed. Clouds and aerosols are not included. The computation was performed under 15th January conditions. Two calculations were carried out with prescribed UV irradiances at the top of the atmosphere for either solar max or solar min conditions according to Lean (2000). As we are only interested in the effect of the different radiation schemes on the resulting heating rates, we only impose UV changes and no solar-induced O_3 variations over the solar cycle. This means that the resulting SW heating rate differences are somewhat smaller than would be the case if SW heating due to solar induced O_3 had been considered as well.

Figure 2 shows SW heating rate differences between solar min and solar max calculated with the FUBRad (top) and the ECHAM5 (bottom) schemes. In FUBRad two peaks occur, one centered at the stratopause summer pole reaching 0.21 K/day, and a second extending over the whole upper summer mesosphere reaching 0.6 K/day. In contrast, the ECHAM5 scheme produces only one peak at the stratopause. With a maximum SW heating rate difference of 0.01 K/day the solar signal in ECHAM5 is about 20 times weaker than in FUBRad. In Fig. 3 we compare the SW heating rate differences of FUBRad and ECHAM5 with those derived from libRadtran for an equatorial profile. Over the full vertical domain of the GCM (up to 0.01 hPa), we find excellent agreement between FUBRad(-TOTAL) and libRadtran, both assuming total conversion of radiative energy to thermal energy. The heating rate differences reach maxima of 0.15 K/day at the stratopause and up to 1 K/day at the mesopause (90 km). Largest differences occur in the upper mesosphere, where FUBRad slightly underestimates solar cycle variability. Heating rate differences between FUB-TOTAL and FUB-NET are

due to the partial conversion of radiative energy to chemical energy and airglow in the upper mesosphere leading to the lower thermal heating in FUBRad-NET. In contrast, ECHAM5 is not able to capture solar cycle variations.

Figure 4 shows the total SW heating rate difference over a solar cycle at 90° S as well as the contributions of the different O_3 and O_2 absorption bands. In the upper mesosphere above about 0.03 hPa the solar signal is dominated by absorption at the Lyman-α wavelength leading to the maximum in SW heating rate differences at the model top of FUBRad (Figs. 3 and 2). As the ECHAM5 scheme does not consider absorption at wavelengths shorter than 250 nm, it does not reproduce the mesospheric maximum. Comparison with libRadtran (not shown) suggests that the contribution from the Schumann-Runge bands and continuum is underestimated in FUBRad by a factor of 2. This explains the deviations in the upper mesosphere in Fig. 3. The maximum of the SW heating rate differences around the stratopause is due to the combined effect in the Herzberg, Hartley, and Huggins absorption bands. While the Hartley bands dominate the SW heating at the stratopause reaching 0.1 K/day, the contribution from the Huggins bands is only half that size and is responsible for the SW heating rate difference at lower altitudes in the stratosphere as also shown by Larkin et al. (2000). The contribution of the Chappuis band is negligible.

5 Temperature response to solar cycle variations

To determine the temperature response caused by the changes in SW heating rates, we have performed two 25-year perpetual January experiments using the FUBRad and ECHAM5 radiation schemes online as submodels of the ECHAM5/MESSy model. We have prescribed the same O_3 climatology and concentrations of uniformly mixed species as in the offline experiments. H_2O and clouds are determined interactively. The model was run at a horizontal resolution of T42 corresponding to a quadratic Gaussian grid of 2.8°× 2.8°, with 39 vertical levels reaching from the ground up to 0.01 hPa (80 km). Note that this version of the model does not produce a self-consistent Quasi-

ACPD
7, 45–64, 2007

Biennial Oscillation (QBO) in the equatorial stratosphere. Solar irradiance at the model top was prescribed using constant solar max and solar min values as described for the offline experiments in Sect. 4.

The differences in zonal mean temperature between the solar max and min experiments are shown in Fig. 5 for January. Consistent with the SW heating rate differences in Fig. 2 temperatures are higher during solar max throughout the atmosphere except for small regions in the troposphere and high NH latitudes for the FUBRad scheme. Statistically significant temperature differences reach 0.5–1 K around the tropical stratopause and throughout the upper stratosphere and lower mesosphere in the Southern (= summer) Hemisphere (SH). The temperature signal at the tropical stratopause is by a few tenths of a degree smaller than in previous simulations with the FUB-Climate Middle Atmosphere Model (FUB-CMAM) (Matthes et al., 2004). This is due to the missing SW heating by enhanced O_3 concentrations during solar max that was ignored in the model setup here. Compared to the FUB-CMAM solar cycle experiments which used the old version of the FUBRad scheme (Matthes et al., 2004), there are two improvements: a stronger and significant warming of the upper mesosphere in summer, replacing the unrealistic cooling of the old model, and a significant warming of the tropical mesopause of 1 K. Both signals can be attributed to the extension of the radiation code by UV absorption in the Lyman-α line. A statistically significant secondary temperature maximum of 0.5 K is located in the tropical lower stratosphere around 20 km. On the winter hemisphere a dipole with positive temperature differences in the upper stratosphere and lower mesosphere and negative temperature differences below is present that is only marginally significant and can be attributed to large interannual variability in the model.

The temperature differences, especially the two tropical maxima are in very good agreement with NCEP-CPC observations (Kodera and Kuroda, 2002) and other model studies with the earlier version of FUB-CMAM (Matthes et al., 2004; their Fig. 4). It must be noted however that due to the different data sources and analysis methods, uncertainties exist in observational estimates of the solar signal which complicate the

validation of the simulated response. E.g. the annual mean solar temperature signal in the upper tropical stratosphere ranges between 0.8 K and 1.75 K in different oberva-tional studies (W. Randel, pers. comm; Crooks and Gray, 2005). Over the thermal wind relationship the simulated temperature differences (Fig. 5) in the upper stratosphere are consistent with a stronger polar night jet during solar max (not shown) apparent also in ERA40-data (Gray et al., 2004).

Again, consistent with the SW heating rate differences in Fig. 2 no statistically signif-icant warming during solar max that is comparable to the simulations with FUBRad and observations can be detected for the ECHAM5 scheme. In contrast to the FUBRad scheme, the simulation with the ECHAM5 scheme shows statistically sig-nificant anomalies only in the NH. Especially prominent is the dipole at polar latitudes that seems to be an internal model feature but not related to solar cycle influences.

6 Conclusions

We have shown that within the vertical domain of the ECHAM5 model, both the 4-band ECHAM5 and the high-resolution FUBRad short wave schemes give heating rates close to those of a detailed radiative transfer code, libRadtran, and should produce realistic results in climate integrations.

For solar cycle simulations, however, a high-resolution radiation scheme is needed. This study demonstrates that the SW part of the solar spectrum needs to be adequately resolved in order to perform realistic solar cycle experiments. The variability in irradi-ance is unequally distributed over the wavelength range with much higher variability at shorter wavelengths. For low-resolution schemes the irradiance changes need to be integrated over a wide spectral range which leads to an underestimation of the variabil-ity in SW heating rates. In our example profile we found 20 times stronger variability in heating rates with the high-resolution parameterization at the stratopause, in very good agreement with a line-by-line calculation. In addition to this, it is essential to include the absorption by O_2 in the Lyman-α band in order to simulate the effect of solar variability

on climate. We have shown that the updated FUBRad parameterization, introduced in this paper, is suitable for realistic solar cycle studies, as the temperature response to solar cycle variations is in good agreement to observations and earlier model studies with the FUB-CMAM model.

The FUBRad scheme is available as a submodel to be used by MA GCMs or CCMs and has been implemented into the ECHAM5/MESSy model for solar cycle studies.

Acknowledgements. We would like to thank M. Giorgetta for providing the offline version of the ECHAM5 radiation code, D. Marsh and D. Kinnison (NCAR, Boulder, USA) for the Lyman-α code, and J. Lean for the spectrally resolved data for the 11-year solar cycle. V. Fomichev and H. Schmidt gave valuable practical advice on different radiation aspects. We particularly thank P. Jöckel for help with the implementation of the FUBRad scheme into the ECHAM5/MESSy model. K. Nissen is supported by the SCOUT-O3 Integrated Project, and K. Matthes by a Marie Curie Outgoing International Fellowship, both within the 6th European Community Framework Programme. Online integrations were performed on the Deutsches Klimarechenzentrum (DKRZ) NEC-SX6 computer.

References

Ackerman, M.: UV-solar radiation related to mesospheric processes, in: Mesospheric models and related experiments, edited by: Fiocco, G., D., Reidel Publishing Company, Dordrecht, 149–159, 1971.

Anderson, G. P., Clough, S. A., Kneizys, F. X., Chetwynd, J. H., and Shettle, E. P.: AFGL atmospheric constituent profiles (0–120 km), AFGL-TR-86-0110, AFGL (OPI), Hanscom AFB, MA 01736, 1986.

Atkinson, R., Baulch, D. L., Cox, R. A., Crowley, J. N., Hampson, R. F., Hynes, R. G., Jenkin, M. E., Rossi, M. J., and Troe, J.: Evaluated kinetic and photochemical data for atmospheric chemistry: Volume I – gas phase reactions of O_x, HO_x, NO_x and O_x species, Atmos. Chem. Phys., 4, 1461–1738, 2004, http://www.atmos-chem-phys.net/4/1461/2004/.

Brasseur, G.: The response of the middle atmosphere to long-term and short-term solar variability: A two-dimensional model, J. Geophys. Res., 98, 23 079–23 090, 1993.

Chabrillat, S. and Kockarts, G.: Simple parameterization of the absorption of the solar Lyman-alpha line, Geophys. Res. Lett., 24, 2659–2662, 1997.
Crooks, S. A. and Gray, L. J.: Characterization of the 11-year solar signal using a multiple regression analysis of the ERA-40 dataset, Climate, J., 18, 996–1015, 2005.
Fleming, E. L., Chandra, S., Jackmann, C. H., Considine, D. B., and Douglas, A. R.: The middle atmosphere response to short and long term solar UV variations: Analysis of observations and 2D model results, J. Atmos. Terr. Phys., 57, 333–365, 1995.
Fortuin J. P. and Langematz, U.: An update on the global ozone climatology and on concurrent ozone and temperature trends, Proceedings of the International Society for Optical Engineering (SPIE): Atmospheric Sensing and Modelling, 2311, 207–216, 1994.
Fouquart, Y., and Bonnel, B.: Computations of solar heating of the earth's atmosphere: A new parameterization, Beitr. Phys. Atmos., 53, 35–62, 1980.
Fröhlich, C.: Observations of irradiance measurements, Space Sci. Rev., 94, 15–24, 2000.
Gray, L. J., Crooks, S., Pascoe, C., Sparrow, S., and Palmer, M.: Solar and QBO Influences on the Timing of Stratospheric Sudden Warmings, J. Atmos. Sci., 61, 2777–2796, 2004.
Haigh, J. D.: The role of stratospheric ozone in modulating the solar radiative effect on climate, Nature, 370, 544–546, 1994.
Haigh, J. D., Blackburn, M., and Day, R.: The Response of Tropospheric Circulation to Perturbations in Lower-Stratospheric Temperature, J. Climate, 18, 3672–3685, 2005.
Jöckel, P., Sander, R., Kerkweg, A., Tost, H., and Lelieveld, J.: Technical Note: The Modular Earth Submodel System (MESSy) – a new approach towards Earth System Modeling, Atmos. Chem. Phys., 5, 433–444, 2005, http://www.atmos-chem-phys.net/5/433/2005/.
Kodera, K.: Solar cycle modulation of the north Atlantic oscillation: Implication in the spatial structure of the NAO, Geophys. Res. Lett., 29, 1218, doi:10.1029/2001GL14557, 2002.
Kodera, K.: Solar influence on the Indian Ocean Monsson through dynamical processes, Geophys. Res. Lett., 31, L24209, doi:10.1029/2004GL020928, 2004.
Kodera, K. and Kuroda, Y.: Dynamical response to the solar cycle, J. Geophys. Res., 107, 4749, doi:10.1029/2002JD002224, 2002.
Larkin, A., Haigh, J. D., and Djavidnia, S.: The effect of solar UV irradiance variations on the Earth's atmosphere, Space Sci. Rev., 94, 199–214, 2000.
Lean, J.: Evolution of the Sun's spectral irradiance since the Maunder Minimum, Geophys. Res. Lett., 27, 2425–2428, doi:10.1029/2000GL000043, 2000.

Lean, J., Rottman, G., Kyle, H., Woods, T., Hickey, J., and Puga, L.: Detection and parameterisation of variations in solar mid- and near-ultraviolet radiation (200–400 nm), J. Geophys. Res., 102, 29 939–29 956, 1997.

Lewis, B. R., Vardavas, I. M., and Carver, J. H.: The aeronomic dissociation of water vapor by solar H Lyman α radiation, J. Geophys. Res., 88, 4935–4940, 1983.

Matthes, K., Kodera, K., Haigh, J. D., Shindell, D. T., Shibata, K., Langematz, U., Rozanov, E., and Kuroda, Y.: GRIPS solar experiments intercomparison project: Initial results, Pap. Meteorol. Geophys., 54, 71–90, 2003.

Matthes, K., Langematz, U., Gray, L. J., Kodera, K., and Labitzke, K.: Improved 11-year solar signal in the FUB-CMAM, J. Geophys. Res., 109, doi:10.1029/2003JD004012, 2004.

Matthes, K., Kuroda, Y., Kodera, K., and Langematz, U.: Transfer of the Solar Signal from the Stratosphere to the Troposphere: Northern Winter, J. Geophys. Res., 111, D06108, doi:10.1029/2005JD006283, 2006.

Mayer, B. and Kylling, A.: Technical Note: The libRadtran software package for radiative transfer calculations: Description and examples of use, Atmos. Chem. Phys., 5, 1855–1877, 2005, http://www.atmos-chem-phys.net/5/1855/2005/.

Minschwaner, K., Anderson, G. P., Hall, L. A., and Yoshino, K.: Polynomial coefficients for calculating O_2 Schumann-Runge cross sections at 0.5 cm^{-1} resolution, J. Geophys. Res., 97, 10 103–10 108, 1992.

Mlynczak, M. G. and Solomon, S.: A detailed evaluation of the heating efficiency in the middle atmosphere, J. Geophys. Res., 98, 10 517–10 541, 1993.

Molina, L. T. and Molina, M. J.: Absolute absorption cross sections of ozone in the 185- to 350-nm wavelength region, J. Geophys. Res., 91, 14 501–14 508, 1986.

Ogawa, S. and Ogawa, M.: Absorption cross sections of $O_2(a^1\Delta_g)$ and $O_2(X^3\Sigma_g^-)$ in the region from 1087 to 1700 Å, Can J. Phys., 53, 1845–1852, 1975.

Roeckner, E., Bäuml, G., Bonaventura, L., Brokopf, R., Esch, M., Giorgetta, M. A., Hagemann, S., Kirchner, I., Kornblueh, L., Manzini, E., Rhodin, A., Schulzweida, U., and Tompkins, A.: The atmospheric general circulation model ECHAM 5. PART I: Model description, MPI-Report 349, 127 pp, 2003.

Sander, S. P., Friedl, R. R., Golden, D. M., Kurylo, M. J., Huie, R. E., Orkin, V. L., Moortgat, G. K., Ravishankara, A. R., Kolb, C. E., Molina, M. J., and Finlayson-Pitts, B. J.: Chemical kinetics and photochemical data for use in atmospheric studies. Evaluation 14, JPL Publication 02–25, Jet Propulsion Laboratory, Pasadena, CA, 2003.

Shibata, K. and Kodera, K.: Simulation of radiative and dynamical responses of the middle atmosphere to the 11-year solar cycle, J. Atmos. Sol.-Terr. Phys., 67, 125–143, 2005.
Stamnes, K., Tsay, S. C., Wiscombe, W., and Jayaweera, K.: A numerically stable algorithm for discrete-ordinate-method radiative transfer in multiple scattering and emitting layered media, Appl. Opt., 27, 2502–2509, 1988.
Strobel, D. F.: Parameterization of the atmospheric heating rate from 15 to 120 km due to O_2 and O_3 absorption of solar radiation, J. Geophys. Res., 83, 6225–6230, 1978.
Woods, T. and Rottman, G.: Solar ultraviolet variability over time periods of aeronomic interest, in Comparative Aeronomy in the Solar System, edited by M. Mendillo, A. Nagy, and J. Hunter Waite, Jr., Geophys. Monograph Series, Wash. DC, pp. 221–234, 2002.
World Meteorological Organization: Atmospheric ozone 1985, Global Ozone Res. Monit. Proj. Rep. 16/1, Geneva, 1986.
Yoshino, K., Parkinson, W. H., Ito, K., and Matsui, T.: Absolute absorption cross-section measurements of Schumann-Runge continuum of O_2 at 90 and 295 K, J. Mol. Spectrosc., 229, 238–243, 2005.
Yoshino, K., Cheung, A. S.-C., Esmond, J. R., Parkinson, W. H., Freeman, D. E.,Guberman, S. L., Jenouvrier, A., Coquart, B., and Merienne, M. F.: Improved absorption cross-sections of oxygen in the wavelength region 205–240 nm of the Herzberg continuum, Planet. Space Sci., 36, 1469–1475, 1988.

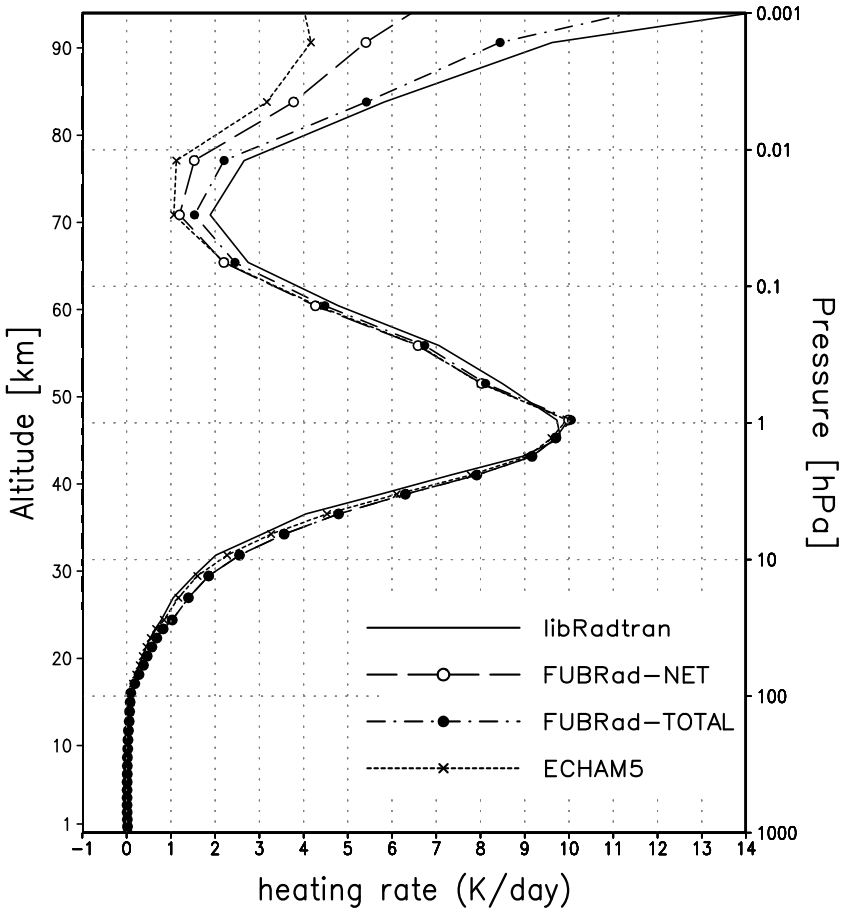

Fig. 1. Daily-mean, short-wave heating rates in K/day for January 15th at the equator. Shown for the spectral interval 121–680 nm for moderate solar irradiance. See text for details.

ACPD
7, 45–64, 2007

EGU

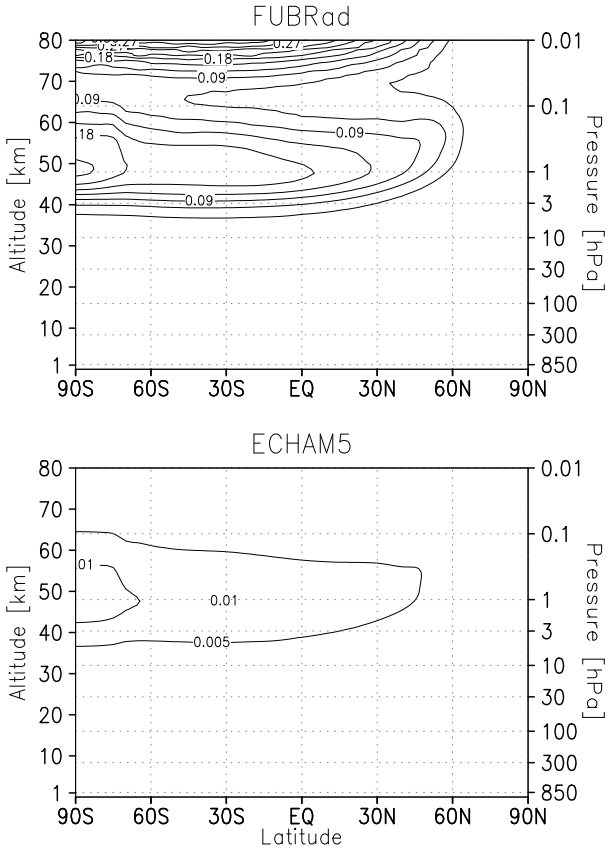

Fig. 2. Daily-mean, zonal-mean short-wave heating rate differences between solar maximum and minimum in K/day for 15 January. Top: FUB radiation scheme, contour interval 0.03 K/day. Bottom: Fouquart and Bonnel radiation scheme, contour interval 0.005 K/day.

ACPD
7, 45–64, 2007

EGU

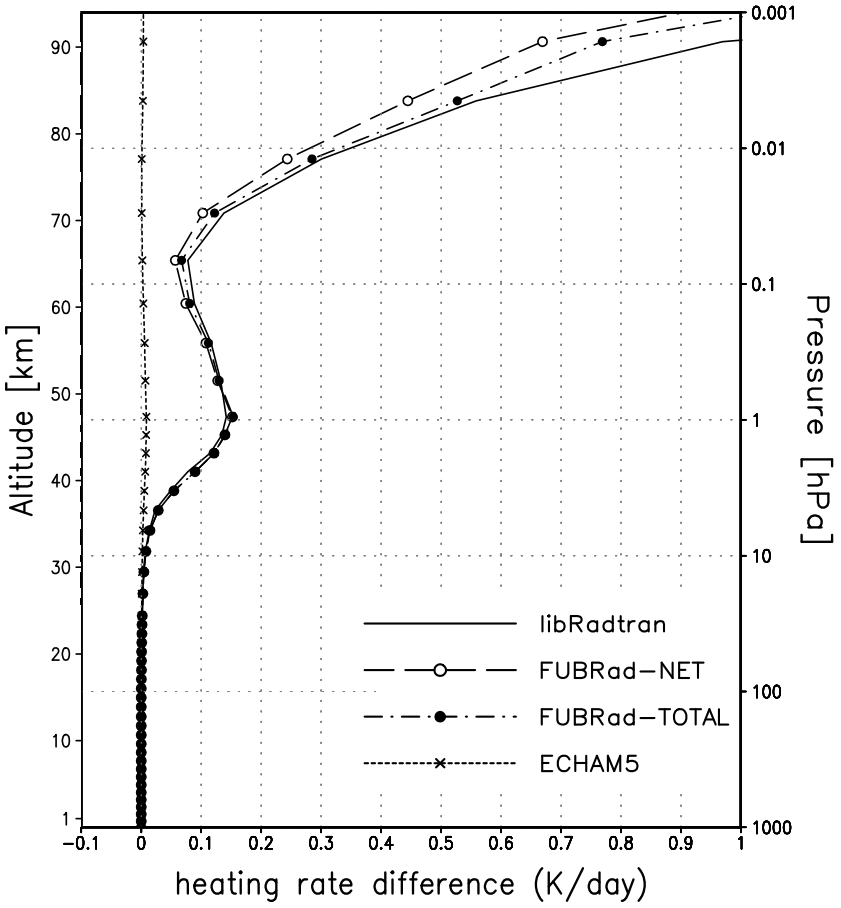

Fig. 3. Difference in daily-mean, short-wave heating rates between solar maximum and solar minimum in K/day. Displayed for 15 January at the equator for the spectral interval 121–680 nm. See text for details.

ACPD
7, 45–64, 2007

EGU

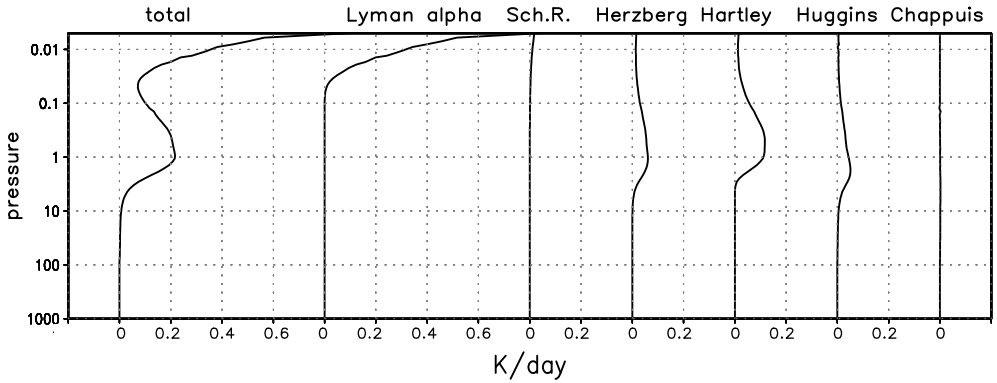

Fig. 4. Differences of short-wave heating rates between solar maximum and solar minimum irradiance in K/day. Daily mean for 15 January at 90° S. Total and contribution of the spectral intervals.

ACPD
7, 45–64, 2007

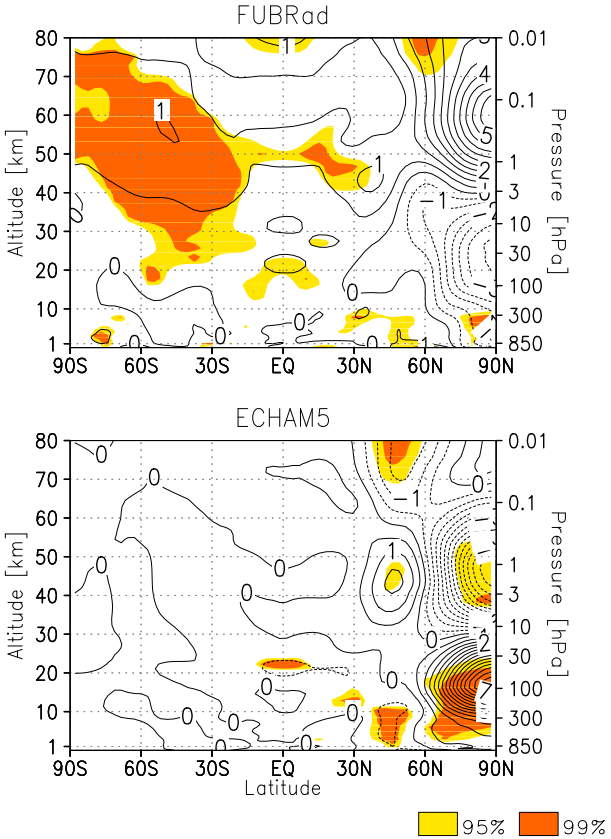

Fig. 5. Longterm-mean temperature difference between solar maximum and solar minimum integration in K. Calculated from perpetual January experiments with the FUBRad (top) and Fouquart and Bonnel (bottom) radiation schemes. Contour interval 0.5 K. Shading: 95% and 99% significance levels, calculated with Student's t-test.